Article

Layered Confinement of Protein in Synthetic Fluorinated Mica via Stepwise Polyamine Exchange

Jiang-Jen Lin, Jiun-Chiou Wei, and Wei-Cheng Tsai

J. Phys. Chem. B, **2007**, 111 (34), 10275-10280 • DOI: 10.1021/jp072973s

Layered Confinement of Protein in Synthetic Fluorinated Mica via Stepwise Polyamine Exchange

Jiang-Jen Lin,* Jiun-Chiou Wei, and Wei-Cheng Tsai

Institute of Polymer Science and Engineering, National Taiwan University, Taipei 10667, Taiwan

Received: April 17, 2007; In Final Form: July 5, 2007

We have developed a process to incorporate the model protein, bovine serum albumin (BSA), into the layered spacing of swelled mica. By a stepwise intercalation, the sodium form of synthetic fluorinated mica (Mica) was first exchanged with the poly(oxyalkylene)-diamine salts (POA-amine) through an ionic exchange reaction and then the BSA embedment. The first step of the Mica space expansion from the pristine 12 Å to 18−93 Å was affected by hydrophobic POP-amines (POP2000 of 2000 g/mol and POP4000 of 4000 g/mol M_w) and the hydrophilic POE2000 that intercalated Na^+-Mica to afford different basal spacing (39, 93, and 18 Å, respectively). The POA modification was necessary for the BSA intercalation and resulted in an uncompressed form of protein conformation in the layered confinement (XRD *d* spacing = 60−71 Å). For comparison, direct intercalation rendered only low *d* spacing (30 Å), in which BSA was embedded in a compressed conformation. The BSA-mica complexes were characterized by X-ray, TGA, and solution analyses. The stepwise process provides a new method for embedding large protein molecules into the clay layered structure generating protein/layered silicate complexes.

Introduction

Utilizing the naturally occurring smectite clays to immobilize proteins is an interesting research approach since the development may lead to practical applications such as bio-sensing for target molecular detection[1] as well as the interface modification for drug delivery[2] and tissue engineering.[3] The conventional methods for protein immobilization may be generally classified as follows: (1) chemical methods by covalent bonding, and (2) physical adsorption by noncovalent bonding interaction between proteins and supports. Both inorganic and organic supports such as porous glass,[4] cellulose,[5] silica gels,[6] and hydrogels[7] are commonly used for these preparations. Particularly, the use of the naturally occurring clays[8] as enzyme supports may have advantages because of their inherent multilayer structure. Hence, both ionic types of clays including anionic layered double hydroxide (LDH) and cationic sodium montmorillonite (Na^+-MMT) are known for their abilities to adsorb biomaterials.[8b,9] The high surface area, ionic character, and layered structure are attractive property features for immobilizing proteins.[10] However, most studies on using clays as the supports have resulted in surface adsorption rather than the clay interlayer encapsulation[8b,8c] or actual intercalation. The difficulty for encapsulating a large molecule into the layered confinement may be caused by the narrow interlayer spacing as well as the inherent adhesive force between the neighboring platelets in the clay structures.

Recently, we have disclosed the use of a family of polyetheramines, including hydrophobic and hydrophilic poly(oxyalkylene)-polyamine salts (POA-amine) of various molecular weights ranging from 230 to 5000 g/mol, for expanding the layered silicates in the XRD basal spacing ranges of 13.5−83.7 Å for Na^+ forms of synthetic fluorinated mica (Na^+-Mica) and 15.0−92.0 Å for the naturally occurring Na^+-MMT.[11] The widening of basal spacing was generally dependent on the increase of molecular weight of the embedded POA organics in a linear manner. The spatial enlargement was generalized for the clays with the ability for cationic exchanging, but their gallery expansion was mainly dominated by their surface charge density and platelet dimension, usually polygonal shapes of 300−1000 nm for Mica[11a] and 80−100 nm for MMT.[11c] Previously, we have found that the BSA model protein could be intercalated into Na^+-MMT in a compressed and uncompressed conformation in the MMT interlayer spacing.[12] The pre-embedded POP-amines may facilitate the accessibility for the BSA intercalation. However, the same technique has encountered a limitation for intercalating the clays of large-platelet dimension, in which surface adsorption was predominant instead of gallery intercalation. To continue the exploration of bio-macromolecular intercalation, here we report the BSA protein encapsulation into the large-platelet Mica.

Experimental Section

Materials. The bovine serum albumin (BSA) (Sigma) in crystalline form is of equilateral triangle shape with a width of 140 Å and a height of 40 Å.[13] In solution, BSA has an isoelectric point (pI) of 4.8, at which the zwitterion charges are balanced.[14] The synthetic fluorinated mica (Na^+-Mica) (trade name of SOMASIF ME-100) has a representative chemical formula of $Na_{0.66}Mg_{2.68}(Si_{3.98}Al_{0.02})O_{10.02}F_{1.96}$ and a cationic exchange capacity (CEC) = 120 mequiv/100 g. The material was obtained from CO-OP Chemical Co. (Japan). A series of poly(oxyalkylene)-diamines (POA-amine) including poly(oxyethylene) (POE)- and poly(oxypropylene) (POP)-backboned diamines of approximately 2000 and 4000 g/mol molecular weight (abbreviated as POE2000, POP2000, and POP4000) are products that are commercially available from Huntsman Chemical Co. The chemical structures are illustrated in Figure 1.

* Corresponding author. Fax: +886-2-3366-5237. E-mail: jianglin@ntu.edu.tw.

10.1021/jp072973s CCC: $37.00
Published on Web 08/09/2007

Hydrophobic Amines

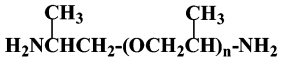

n = 33 (M_w = 2000; POP2000)

n = 68 (M_w = 4000; POP4000)

Hydrophilic Amine

a+c = 5, b = 39.5 (M_w = 2000; POE2000)

Figure 1. Chemical structures of hydrophobic poly(oxypropylene)- and hydrophilic poly(oxyethylene)-diamines of various molecular weights for the Mica intercalation.

Preparation of POA-Amine Intercalated Micas and Their Lower Critical Solution Temperature (LCST)[15] Measurements. The preparation of the POP2000-, POP4000-, and POE2000-intercalated Na^+-Mica and Na^+-MMT has been reported previously.[11a] A typical experimental procedure is described below. Na^+-Mica (3 g, 120 mequiv/100 g) was placed in a 1 L beaker, 300 mL of deionized water was added, the mixture was vigorously stirred by a mechanical stirrer, and the contents were heated to 80 °C for several hours. In a separate vessel, the intercalating amine (POP2000, 7.2 g, 3.6 mmol) was acidified with hydrochloric acid (37% in water, 3.6 mmol, acidification ratio of $H^+/NH_2 = 1/2$). The solution was then poured into the vessel containing the swelled Na^+-Mica slurry. The mixture was stirred vigorously at 80 °C for 5 h and then allowed to cool to room temperature. The resulting agglomerated precipitate was collected, washed thoroughly with deionized water to remove free amines, and dried in a vacuum oven at 80 °C for 24 h. The X-ray diffraction analyses showed *d* spacing of 41.6, 68.2, and 18.0 Å for the samples of POP2000-Mica, POP4000-Mica, and POE2000-Mica, respectively. The POP-amine intercalated Mica hybrids have shown characteristics of increasing solubility by decreasing temperature, similar to the behaviors of nonionic surfactants' lower critical solubility temperature (LCST). The hybrids were dispersible in water in the temperature range of 5−30 °C, but largely aggregated and phase separated from water at a temperature higher than 30 °C. Hence, the intercalation was required to be performed at a temperature lower than the LCST, preferably at 4 °C. The LCST was determined by measuring the turbidity or the optical absorption at 550 nm at the hybrid concentration of 3 mg/mL in water.

Adsorption and Intercalation of BSA. The experiments of adsorption and intercalation were performed in various pH buffer solutions, adjusted by the formic buffer (formic acid and KOH) for 2.0 < pH < 6.0 and in phosphate buffer (KH_2PO_4 and Na_2HPO_4) for 6.0 < pH < 9.0. In all cases, the pH solution may be further adjusted to the desired value by the addition of 0.5 M NaOH or HCl. The suspensions of 30 mg/mL of BSA and 15 mg/mL of Na^+-Mica were prepared separately as stock solutions. To the specific buffer solution, the Na^+-Mica (60 mg) and the BSA at varied volume (60−240 mg) was introduced in that order into a beaker and the final volume was kept at 40 mL. The suspensions of the protein/clay (w/w) at the weight ratios of 1, 2, 3, and 4 were well mixed and maintained at 4 °C for 24 h. The suspensions were then centrifuged for 10 min at 10 000 rpm and washed twice with distilled water to remove free proteins.

Instruments and Analyses. The protein concentration in the supernatant was measured by UV absorption at $\lambda = 280$ nm according to a standard curve, which was found to be free of POP-amine interference. The amount of BSA adsorbed per gram of mica was calculated by the difference of the BSA concentration in water before and after the process. The temperature effects on the POP2000 solubility and the aggregation of the POP2000-intercalated Mica were determined with a Jasco V-530 UV−visible spectrophotometer by measuring their transmittance at 550 nm wavelength. The XRD patterns were obtained with a powder diffractometer (Schimadzu SD-D1 using a Cu target at 35 kV, 30 mA). The *d* spacing was calculated according to Bragg's equation ($n\lambda = 2d \sin\theta$) by fitting the series of θ values to find the $n=1$ *d* spacing. The TGA patterns were obtained with a thermal gravimetric analysis (Perkin-Elmer Pyris 1) by heating the samples from 100 to 900 °C at 10 °C/min in air.

Results and Discussion

Fundamental Properties of Na^+-Mica and the POA-Modified Mica. The naturally occurring mica is not swelled in water due to the inherent property of cross-linking hydroxyl sheets. However, the synthetic mica, derived from the Na_2SiF_6 treatment of natural micas, is dispersible in water and ionically exchangeable with organic amine salts.[16] The sodium form of the synthetic fluorinated mica (Na^+-Mica) has an irregular polygonal shape of 300−1000 nm[11a] and relatively higher aspect-ratio than the commonly utilized Na^+-MMT (80−100 nm).[11c] Previously, the intercalation of poly(oxyalkylene)-amine salts (POA-amine) for MMT and Mica clays to prepare the hybrids of POA-MMT and POA-Mica has been studied.[11] The hydrophobic POP-amines (POP2000 of 2000 g/mol and POP4000 of 4000 g/mol M_w) and the hydrophilic POE2000, structures shown in Figure 1, may intercalate with Na^+-Mica to afford different basal spacing (39, 93, and 18 Å, respectively). The organically modified clays were shown to have distinctly different hydrophobic or hydrophilic characters from their pristine Na^+-Mica. With the POP-amine intercalation, the resultant POP2000- and POP4000-Mica were actually hydrophobic and precipitated out from water at ambient temperature. In contrast, the pristine Na^+-Mica and the POE2000-Mica were water-dispersible.[11a]

pH-Dependent BSA Adsorption and Intercalation. Owing to the presence of anionic charges on the mica surface (≡SiO−Na^+ for Na^+-Mica and ≡SiO−N^+ for the POP-Mica), the adsorption of BSA onto the clay surface may be predominant in a kinetic sense driven by the balance of surface charges of the clay and the charges on the protein in an aqueous medium of a specific pH. The amount of protein adsorbed and intercalated with the silicate Mica was influenced by the pH changes. In an acidic medium (pH < 4.8), the amine groups existed as amine salts which were then possibly exchanged and intercalated with the metal ions within the clay interlayer. Hence, the different pH mediums affect the ionic character of BSA molecules and consequently the way of interacting with the clay. As shown in Figure 2, the effect of pH on the amounts of BSA adsorption is demonstrated. The pristine Na^+-Mica and its POP-amine-salt modified mica (POP2000-Mica) were allowed to interact with BSA at various pH values below or above the BSA isoelectric point (pI) of 4.8. At a pH above the pI, the BSA carries negative charges (−COO−). Hence, with increasing pH > pI, the BSA may associate with the Na^+ counterions on the clay surface in Na^+-Mica and POP2000-Mica. In the range of

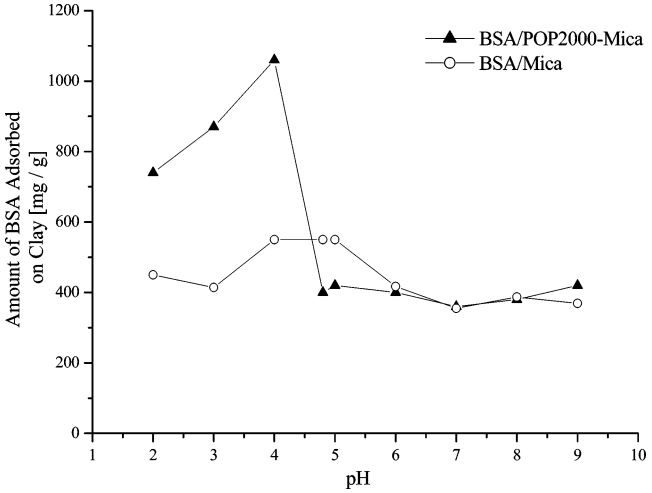

Figure 2. Relative adsorption ability of BSA on Na^+-Mica and POP2000-Mica at different pH values.

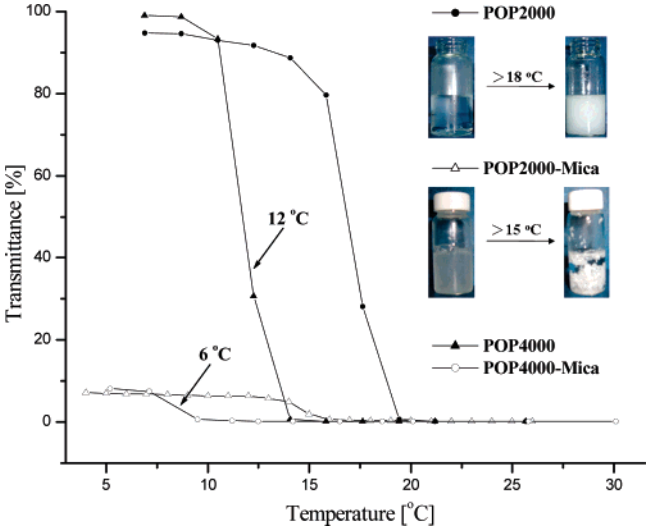

Figure 3. Lower critical aggregation temperature of the POP2000- and POP4000-modified Mica, POP2000- and POP4000-diamine, and Na^+-Mica.

pH 4.8−9.0, the BSA was measured to be adsorbed in the amount of only 400 mg per gram of clay. In contrast, at pH < pI, BSA is mostly positively charged (or in the form of $-NH_3^+$) and suitable for adsorption on the surface and also ionic exchange (intercalation) with $\equiv SiO-Na^+$ in the silicate galleries. The sharp increase in adsorption at pH 4 (ca. 1000 mg/g) suggests the optimal pH value for the clay interaction.

Temperature-Dependent Intercalation Process Involving an Inverse Temperature Factor. Besides the condition of pH environment, the suitable temperature for the BSA intercalation was optimized in considering that the POP-intercalated Mica actually possesses an inverse temperature factor when dispersing in water. It was observed that the dispersion ability diminished when the temperature increased. Previously, it was shown that, with the POP2000 or POP4000 intercalation, the pristine Na^+-Mica clay shifted its dispersing ability and water-swollen property by the influence of POP organics. The hybrid actually exhibited both hydrophilic and hydrophobic character (amphiphilic) since the hybrids are comprised of ionic character as well as the hydrophobic POP2000- and POP4000- organic fractions. It is known that the original POP-amines have the characteristics of lower critical solution temperature (LCST) below the ambient temperature, as measured by the optical absorption at 550 nm at the concentration of 3 mg/mL in water. As shown in Figure 3, POP2000 was soluble only at a critical temperature below 18 °C. Above the temperature, the breaking of hydrogen bonding interaction occurs and the POP solubility in water decreases. Similarly, the POP4000 diamine possesses a LCST at 12 °C. When the POP is embedded in the silicate interlayer, the hybrids (*d* spacing at 39 and 93 Å for POP2000-Mica and POP4000-Mica, respectively) were affected by the presence of POP organics and rendered an inverse temperature factor for the ease of dispersion in water. Consequently, the hybrids had a higher dispersing ability at temperatures lower than 25 °C. This unique dispersion property is caused by the presence of POP-amine existing in the silicate galleries; hence, it can be considered as the "lower critical aggregation temperature" or LCAT.[12] When measured by the relative optical transparency in water, the POP2000-Mica and POP4000-Mica were shown to have a significant change in the transmittance at 15 and 6 °C, respectively. The change of sudden precipitation was visible with the naked eye as recorded in the inserted pictures in Figure 3. For comparison, the pristine Na^+-Mica and the hydrophilic POE2000-Mica remained at constant transmittance throughout the range from 5 to 30 °C without the observation of LCAT. The presence of POP organics facilitates

SCHEME 1: Conceptual Illustration of BSA Intercalation into Na^+-Mica Directly and the Amine Salt-Modified Mica under the Same Conditions of pH = 4 and 4 °C

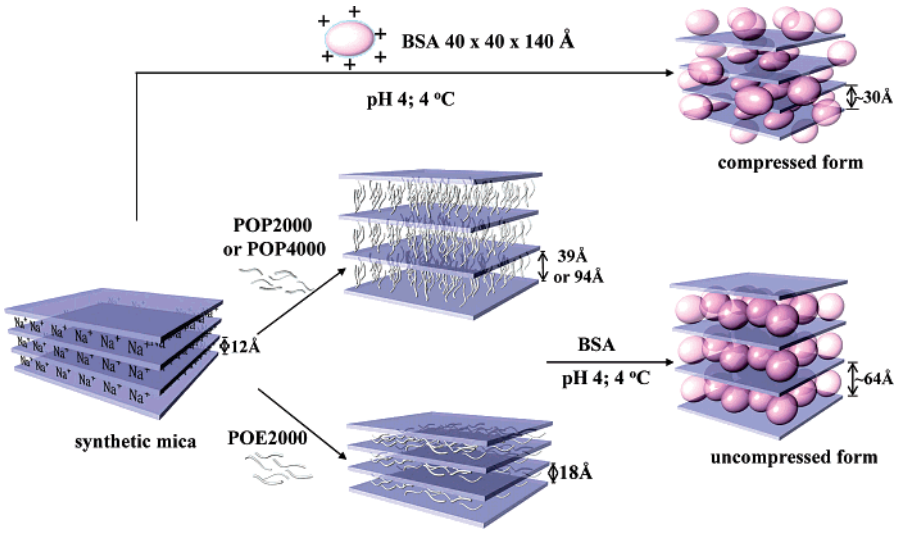

TABLE 1: Embedding of BSA into Layered Silicates with and without the POP- or POE-Amine Modifications

	BSA adsorption				
		weight fraction (org/inorg)			
weight ratio of BSA/Mica[a]	adsorbed (mg/g Mica)	adsorbed[b]	actual[c]	*d* spacing XRD (Å)[d]	dispersibility in water[e]
		Na^+-Mica			
0/1	0		9/91	12	+
1/1	340	33/67	25/75	N.D.[f]	+
2/1	510	39/61	26/74	N.D.	+
3/1	680	43/57	27/73	N.D.	+
4/1	830	51/49	35/65	30	+
		POP2000-Mica			
0/1	0		51/49	39	−
1/1	960	49/51	56/44	49	+
2/1	1260	56/44	59/41	58	+
3/1	1430	59/41	59/41	60	+
4/1	1600	62/38	61/39	60	+
		POE2000-Mica			
0/1	0		38/62	18	+
1/1	920	48/52	41/59	29	+
2/1	1100	52/48	47/53	62	+
3/1	1300	57/43	47/53	64	+
4/1	1600	62/38	52/48	64	+
		POP4000-Mica			
0/1	0		82/18	93	−
1/1	300	23/77	80/20	93	−
2/1	560	36/64	79/21	93	−
3/1	720	42/58	77/23	93	−
4/1	800	45/55	77/23	93	−
10/1	2030	68/32	71/29	71	+

[a] Experiments were preformed by using 15 mg/mL mica as the starting materials and the corresponding amount of BSA weight. [b] Weight ratios of BSA to mica based on the BSA concentration in aqueous solution. [c] Based on TGA measurements. [d] XRD $n = 1$ basal spacing is calculated according to the Bragg's equation ($n\lambda = 2d \sin\theta$). [e] +: dispersible; −: aggregated. [f] N.D.: not detectable.

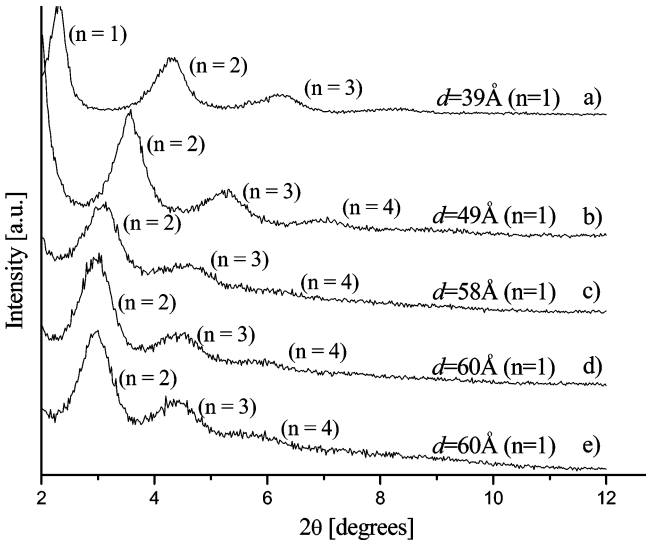

Figure 4. X-ray Bragg's patterns of the BSA-intercalated Micas, prepared from (a) POP2000-Mica at pH 4.0, (b) BSA/POP2000-Mica = 1/1, (c) BSA/POP2000-Mica = 2/1, (d) BSA/POP2000-Mica = 3/1, and (e) BSA/POP2000-Mica = 4/1.

the formation and the breaking of hydrogen bonding between POP and water. The existence of a LCAT phenomenon implied that the BSA interaction should be performed below 6 °C.

Intercalation or Adsorption of BSA with POA-Mica Hybrids—Stepwise Process. The interaction of BSA and Mica resulted in two types of protein embedment into the clay gallery

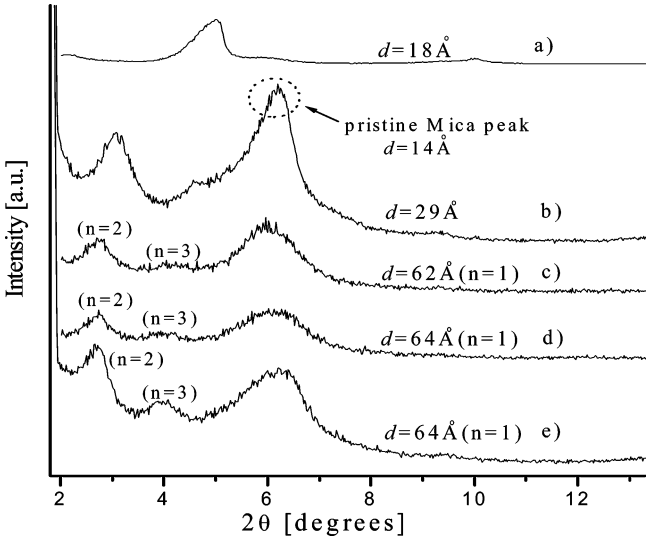

Figure 5. X-ray Bragg's patterns of the BSA-intercalated Mica, prepared from (a) POE2000-Mica at pH 4.0, (b) BSA/POE2000-Mica = 1/1, (c) BSA/POE2000-Mica = 2/1, (d) BSA/POE2000-Mica = 3/1, and (e) BSA/POE2000-Mica = 4/1.

in addition to the adsorption onto the surface. In Scheme 1, the conceptual diagram illustrates two types of BSA-Mica intercalation: the compressed and the uncompressed forms. Analyses of X-ray diffraction actually revealed more than one type of silicate interlayer *d* spacing after the intercalation. The direct intercalation of BSA into Na^+-Mica was found to have a maximal 30 Å and organic embedment of 25−35% in composition (Table 1). It was noted that the pristine Na^+-Mica had an original 12 Å XRD *d* spacing, implying only a 2 Å space distance between two neighboring platelets (i.e., XRD diffraction subtracts the platelet thickness of 10 Å). This estimated gallery space is much narrower than the possible BSA dimension (40 × 40 × 140 $Å^3$).[12] Apparently, the direct intercalation failed to generate an interlayer space for embedding the large size of protein conformation or only allowed a compressed form of BSA in the Mica galleries in a low spacing. The result was different from that of BSA intercalation with Na^+-MMT, which could be intercalated by BSA under the process condition of high BSA concentration.[12]

The alternative process involving the stepwise POA-amine-salt and BSA intercalation into the Mica gallery was explored. Na^+-Mica was first intercalated by using a series of poly(oxyalkylene)-amine salts (POA-amine) to enlarge the interlayer spacing. The spatially enlarged spacing allowed the accessibility for the incoming large organic molecules. In the case of POP2000 intercalation with Mica, the resultant POP2000-Mica had an enlarged *d* spacing of 39 Å from the pristine 12 Å of Na^+-Mica. In the second step, the POP-Mica hybrid was exchanged with BSA to afford new hybrids with *d* spacing of 49, 58, 60, and 60 Å, depending on the amount of BSA in relation to the Mica at 1/1, 2/1, 3/1, and 4/1 weight ratios, respectively (Figure 4). The XRD *d* spacing expansion from 39 to 60 Å is a good indication of the BSA replacement with POP2000. Besides the XRD analyses, the solution analysis by simple gel permeation chromatography showed that a significant amount of POP organics was released from the insoluble silicates. The XRD basal spacing of 60 Å is approximated to be 50 Å for the gallery width between two platelets (after subtracting the 10 Å platelet thickness). The interlayer spacing is in good agreement with the dimension of BSA (40 Å in one dimension). Furthermore, with the increasing amount of BSA addition, the hybrids had slightly more expansion (Table 1).

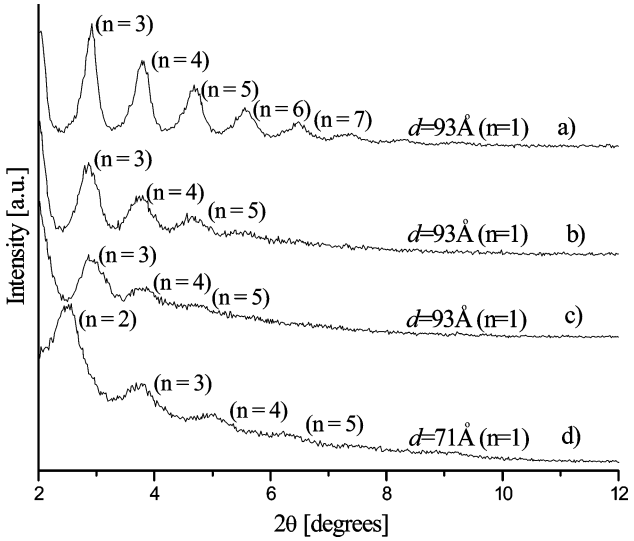

Figure 6. X-ray Bragg's patterns of the BSA-intercalated Mica, prepared from (a) POP4000-Mica at pH 4.0, (b) BSA/POP4000-Mica = 1/1, (c) BSA/POP4000-Mica = 4/1, and (d) BSA/POP4000-Mica = 10/1.

Perhaps the BSA molecules were aggregated in a bilayer orientation in the gallery through further ionic interaction or water association. The bilayer intercalation may result in the clay expansion being slightly higher than the primary monolayer thickness of the BSA molecules.

In order to understand the intercalating mechanism, the hydrophobic POP4000 and hydrophilic POE2000 were used for the Mica intercalation. The hybrids were analyzed to have the original XRD *d* spacing of 93 and 18 Å, respectively. The distinct difference between the POP- and POE-amine intercalation in expanding the silicate galleries was previously reported.[11] The exceptionally high spacing for POP4000 was attributed to the generation of a hydrophobic aggregation in the silicate gallery, while the polar POE could only associate with the platelet surface through the $-(CH_2CH_2O)_{x-}/Na^+$ interaction rather than a hydrophobic phase separation. However, when the BSA was allowed to exchange with POE2000-Mica (18 Å *d* spacing), the Mica was converted into the *d* spacing of 29, 62, 64, or 64 Å depending on the BSA loadings to Mica at 1/1, 2/1, 3/1, and 4/1 ratios, respectively (Figure 5). This series of intercalation implies the progressive BSA embedment from the compressed conformation of 29 Å *d* spacing to the uncompressed conformation in the 64 Å *d* spacing, or an actual 54 Å interlayer distance by subtracting the 10 Å platelet thickness from the XRD *d* spacing. The enlargement has reached a hybrid which is similar to that obtained from the POP2000-Mica exchange. For the BSA exchange with the original high-spacing POP4000-Mica, the hybrid remained a high XRD *d* spacing but the pattern of the XRD Bragg's peaks (from $n = 2$ to 7) became less regular and peaks broader, at increasing amounts of BSA from 1/1 to 4/1 weight ratios (Figure 6b,c). Only at a large excess of BSA amount (10/1 weight ratio to Mica), was the significant decrease in *d* spacing from 93 to 71 Å observed, which spacing is more reflective of the dimensional size of the protein. It was envisioned that the BSA exchange occurred incrementally with the POP4000 organics and finally the complete replacement of BSA with POP. The resultant 71 Å hybrid had a different characteristic of solvophilicity in water. The new BSA-Mica hybrid is evidenced since the new hybrid became highly hydrophilic in nature and lacked the LCST behavior that originally existed for the POP-Mica hybrids.

All XRD analyses indicated that BSA may intercalate into the galleries of the Mica by exchanging with the hydrophobic POP2000, POP4000, or the hydrophilic POE2000. As illustrated in Scheme 1, the BSA replacement with either type via hydrophobic POP- or hydrophilic POE-Mica hybrids afforded the same result for the BSA incorporation into the Mica galleries. By comparison, the direct BSA intercalation with Na^+-Mica failed to incorporate the free form of BSA molecules. Previously, we have reported the direct incorporation of BSA into Na^+-MMT[12] at a high *d* spacing of 62 Å. The difficulty in intercalating BSA with Na^+-Mica is attributed to the steric hindrance for the large Mica platelets.

Thermal Stability of BSA in Silicate Confinement. By using thermal gravimetric analysis, the hybrids with different thermal degradation patterns could be differentiated and correlated with the BSA intercalation or just an adsorption onto the Mica surface. The POP-intercalated Mica had only a single decomposition slope around 250−350 °C for the organics (Figure 7a). In comparison, BSA exhibited at least two decomposition rates in the temperature ranges of 200−400 °C and 550−650 °C. The similar two-slope pattern was observed in the BSA-Mica hybrids, implying the actual BSA replacement with POP-amine. Another difference in Figure 7a was shown to have a lower decomposition temperature ($T_d = 215$ °C) for the BSA-Mica after the replacement with POP2000-Mica than the pristine BSA ($T_d = 260$ °C). In our previous study[12] on the

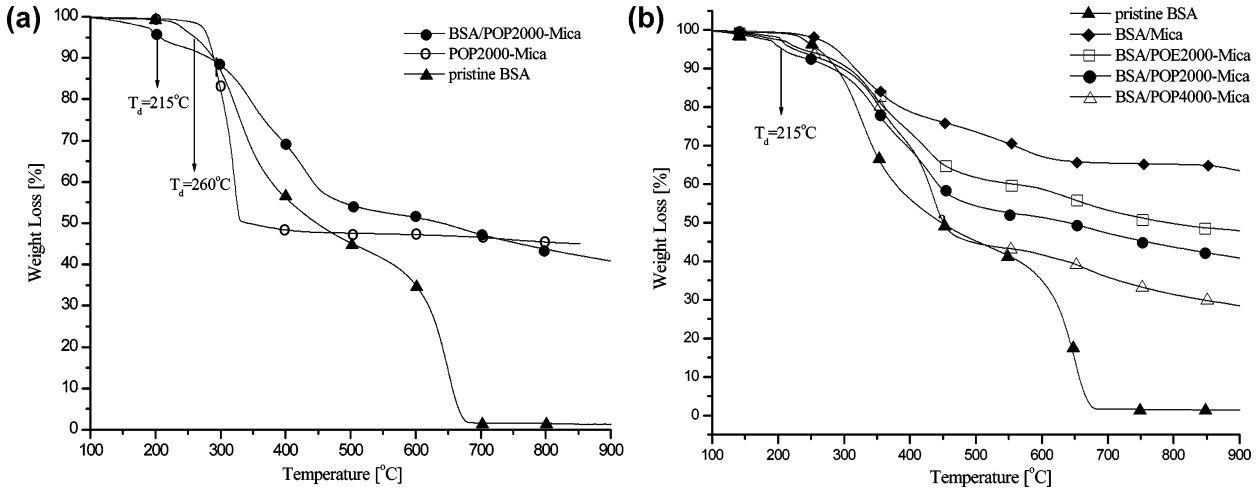

Figure 7. Thermo-oxidative degradation patterns of BSA-intercalated Mica (4/1 weight ratio), (a) pristine BSA and POP2000-Mica, and (b) pristine BSA and the different modified Mica.

BSA intercalation with Na^+-MMT, there was no evidence for showing the faster decomposition for the BSA in the clay. Perhaps the difference in the clay species between Mica and MMT may affect the BSA cracking. The presence of the fluorine ion in the Mica silicates may contribute to the pattern of organic cracking. In the differentiation of the BSA embedment in the clay gallery or absorption on the silicate surface, TGA analyses had shown a noticeable difference in the cracking patterns. Only in the form of BSA intercalation from POP-Mica (XRD d = 48−71 Å), was the earlier cracking pattern observed but not in the BSA direct intercalation of Mica (BSA/Mica in Figure 7b).

Conclusion

The stepwise intercalation was effective for encapsulating the BSA protein into the inorganic Mica interlayer galleries of 49−71 Å d spacing. Three representative poly(oxyalkylene)-diamines, hydrophilic POE2000- and hydrophobic POP2000- and POP4000-diamine were allowed to intercalate at 18, 39, and 93 Å XRD basal spacing, respectively. The second intercalation with BSA, performed at the temperature below their LCAT (6−15 °C) dispersing temperatures, could generate the free form of BSA embedment. By comparison, the direct BSA intercalation toward Na^+-Mica can only achieve a low d spacing of 30 Å, presumably a compressed BSA conformation. The use of the POA-amine-modified Mica is necessary to achieve an uncompressed BSA in the confinement. The TGA data further provided evidence for the actual BSA embedment in the gallery. The stepwise process may allow an efficient way to incorporate BSA into the large-platelet Mica clays and may be potentially useful for biomedical applications.

Acknowledgment. National Science Council (NSC) of Taiwan.

References and Notes

(1) (a) Zen, J. M.; Lo, C. W.; Chen, P. J. *Anal. Chem.* **1997**, *69*, 1669. (b) Zen, J. M.; Kumar, A. S. *Anal. Chem.* **2004**, *76*, 205A.

(2) (a) Jayakrishnan, A.; Jemeela, S. R. *Biomaterials* **1996**, *17*, 471. (b) Gan, Q.; Wang, T.; Cochrane, C.; McCarron, P. *Colloid Surf. B*—Biointerfaces **2005**, *44*, 65.

(3) Tsai, C. C.; Chang, Y.; Sung, H. W.; Hsu, J. C.; Chen, C. N. *Biomaterials* **2001**, *22*, 523.

(4) (a) Ressine, A.; Ekstrom, S.; Marko-Varga, G.; Laurell, T. *Anal. Chem.* **2003**, *75*, 6968. (b) Mansur, H. S.; Lobato, Z. P.; Orefice, R. L.; Vasconcelos, W. L.; Oliveira, C.; Machado, L. J. *Biomacromolecules* **2000**, *1*, 789. (c) Shriver-Lake, L. C.; Gammeter, Wm. B.; Bang, S. S.; Pazirandeh, M. *Anal. Chim. Acta* **2002**, *470*, 71.

(5) Kauffmann, C.; Shoseyov, O.; Shpigel, E.; Bayer, E. A.; Lamed, R.; Shoham, Y.; Mandelbaum, R. T. *Environ. Sci. Technol.* **2000**, *34*, 1292.

(6) Shchipunov, Y. A.; Karpenko, T. Yu.; Bakunina, I. Yu.; Burtseva, Y. V.; Zvyagintseva, T. N. *J. Biochem. Biophys. Methods* **2004**, *58*, 25.

(7) Dumitriu, S.; Chornet, E. *Adv. Drug Delivery Rev.* **1998**, *31*, 223.

(8) (a) Peng, S.; Gao, Q.; Wang, Q.; Shi, J. *Chem. Mater.* **2004**, *16*, 2675. (b) De Cristofaro, A.; Violante, A. *Appl. Clay Sci.* **2001**, *19*, 59. (c) Naidja, A.; Huang, P. M.; Bollag, J. M. *J. Mol. Catal. A: Chem.* **1997**, *115*, 305.

(9) Shan, D.; Yao, W.; Xue, H. *Electroanalysis* **2006**, *18*, 1485.

(10) Giannelis, E. P. *Adv. Mater.* **1996**, *8*, 29.

(11) (a) Lin, J. J.; Chen, Y. M. *Langmuir* **2004**, *20*, 4261. (b) Lin, J. J.; Chen, I. J.; Chou, C. C. *Macromol. Rapid Commun.* **2003**, *24*, 492. (c) Chou, C. C.; Shieu, F. S.; Lin, J. J. *Macromolecules* **2003**, *36*, 2187−2189.

(12) Lin, J. J.; Wei, J. C.; Juang, T. Y.; Tsai, W. C. *Langmuir* **2007**, *23*, 1995.

(13) Musale, D. A.; Kulkarni, S. S. *J. Membr. Sci.* **1997**, *136*, 13.

(14) Cao, C. X.; Zhang, W.; Qin, W. H.; Li, S.; Zhu, W.; Liu, W. *Anal. Chem.* **2005**, *77*, 955.

(15) (a) Gil, E. S.; Hudson, S. M. *Prog. Polym. Sci.* **2004**, *29*, 1173. (b) Mao, H.; Li, C.; Zhang, Y.; Bergbreiter, D. E.; Cremer, P. S. *J. Am. Chem. Soc.* **2003**, *125*, 2850.

(16) Kodama, T.; Higuchi, T.; Shimizu, K. I.; Komarneni, S.; Hoffbauerd, W.; Schneider, H. *J. Mater. Chem.* **2001**, *11*, 2072.